JOURNAL OF Applied Polymer SCIENCE

Curing Studies of Bisphenol A Based Bismaleimide and Cloisite 15a Nanoclay Blends Using Differential Scanning Calorimetry and Model-Free Kinetics

R. Surender,[1,2] A. Mahendran,[3] A. Thamaraichelvan,[1] S. Alam,[4] C. T. Vijayakumar[2]

[1]Postgraduate and Research Department of Chemistry, Thiagarajar College, Madurai 625 009, India

[2]Department of Polymer Technology, Kamaraj College of Engineering and Technology, S. P. G. C. Nagar, K. Vellakulam Post 625 701, India

[3]Wood Carinthian Competence Centre, Kompetenzzentrum Holz GmbH, Klagenfurterstrasse 87–89, A-9300 Sankt Veit an der Glan, Austria

[4]Defence Materials and Stores Research and Development Establishment, G. T. Road, Kanpur 208 013, India

Correspondence to: C. T. Vijayakumar (E-mail: ctvijay22@yahoo.com)

ABSTRACT: Blends of 2,2-bis[4-(4-maleimidophenoxy phenyl)]propane [bismaleimide (BMIX)] with different proportions (1, 2, 3, 4, 5, 7, and 9%) of the nanoclay Cloisite 15a were prepared with ultrasonication. Fourier transform infrared studies reveal the existence of interactions between the clay particles and the imide rings in BMIX. The difference in the melting characteristics and the decrease in the curing window caused by the incorporation of the clay particles in BMIX, as evidenced by detailed differential scanning calorimetry investigations, confirmed the existence of interactions between the nanoclay particles and BMIX molecules. The Flynn–Wall–Ozawa, Vyazovkin, and Friedman kinetics methods were used to calculate the activation energies (E_a's) for the curing of the BMIX materials. E_a for the polymerization varied, depending not only on the amount of clay loaded in the BMIX but also on the extent of the curing reaction. Because of the loss of interaction between the clay platelets and the imide rings of BMIX, a decrease in E_a at higher reaction extents was noted when there was lower clay loadings (1–4% Cloisite 15a) in BMIX. A reversal in the previous behavior was noted at higher clay loadings (7 and 9% Cloisite 15a) in BMIX and was attributed to the restriction of the molecular mobility due to the presence of increased concentrations of clay platelets and the decreased availability of reaction sites for polymerization. These two opposing factors played were equal at the optimum level of Cloisite 15a loading (5%) in BMIX, which was reflected in the constancy of E_a variation noted with increasing reaction extent. © 2012 Wiley Periodicals, Inc. J. Appl. Polym. Sci. 000: 000–000, 2012

KEYWORDS: blends; differential scanning calorimetry (DSC); kinetics; nanocomposites; spectroscopy

Received 3 November 2011; accepted 18 June 2012; published online

DOI: 10.1002/app.38219

INTRODUCTION

Most high-performance materials are produced with thermosetting materials, and the properties of these materials depend on the extent of chemical reactions during the curing process. The heat liberated during the curing process accelerates the curing rates of the material.[1] A small amount of nanoparticles in the polymer matrix alter the mechanical, thermal, and optical properties of the material.[2] Polymer nanocomposites are prepared with five synthetic methods: (a) *in situ* polymerization, (b) direct melt intercalation, (c) solution intercalation, (d) the direct layered silicate method, and (e) the dispersion and aggregation method.[3] Polyimide is a condensation polymer (produced from acid anhydrides and primary amines) having outstanding properties, such as thermooxidative stability, high mechanical strength, high modulus, excellent chemical resistance, and electrical properties.[4]

Differential scanning calorimetry (DSC) is one of the techniques used to investigate different thermal properties, including melting, crystallization, curing, and glass-transition temperature (T_g), of polymer nanocomposites.[2] It is essential to understand the kinetics of the curing reaction to understand and control heat generation during the curing reaction and to process the materials. Normally, layered silicate nanoparticles are used as nanofillers for polymer nanocomposites. To prevent the agglomeration of clay particles in the polymer matrix, the surface of the clay should be organically modified, and such materials are

referred to as *organoclays*. The exchange of interlayer cations is the most popular modification method and may increase the interlayer spacing and reduce the interlayer attractions of the clay platelets. The modification may affect the curing process of the matrix system through the steric effect of the clay.[5]

Montmorillonite clay is the most commonly used layered silicate system for the preparation of polymer nanocomposites because of its larger active surface area (700–800 m^2/g) and moderately negative surface charge (cation-exchange capacity). To increase the *d*-spacing between the clay layers, ion-exchange reactions are carried out, and hydrocarbon groups of varying sizes are grafted onto the clay layers. Normally, alkyl ammonium salts are used to replace the cations from layered silicates to impart hydrophobic/organophilic characteristics; this typically results in a large interlaying spacing. The negative charge originates in the layered silicate, and the cationic head groups of the alkyl ammonium chloride molecule preferentially reside at the surface of the layered silicate (i.e., the quaternary ammonium chloride portion in the surfactants interact with the silicate surface), whereas the oligomeric tallow species, which sometime contain polar groups, extend into the galleries.[6,7] Cloisite 15a is an organically modified montmorillonite system in which the clay layers are modified with dimethyldihydrogenated tallow quaternary ammonium salt. The hydrogenated tallow consists of about 65% C18, about 30% C16, and about 5% C14. It should be mentioned that 100% of Na^+ ions in natural montmorillonite have been exchanged.[8] The *d*-spacing of the montmorillonite clay is around 10 Å without any water layers[9] and is around 31.5 Å for the Cloisite 15a clay layers.[10]

Parthasarathy et al.[11] investigated polyethylene nanocomposites with Cloisite 15a and observed that the strong interactions of clay particles led to significant increases in the viscosity and tensile strength. Ersali et al.[12] studied the properties of ethylene–propylene–diene monomer/acrylonitrile butadiene rubber/organoclay (Cloisite 20A) nanocomposites. The clay particles decreased the curing time and increased the abrasion resistance. The kinetic parameters of the curing of an epoxy blended with Cloisite 30B were studied by Ngo et al.,[5] and there were no significant changes in the activation energies (E_a's) for a Cloisite-blended epoxy matrix compared to their neat resin.

The physical and mechanical properties of butyl rubber with montmorillonite organoclay (Cloisite 15a) were studied by Razzaghi-Kashani et al.[10] The organoclay Cloisite 15a was mixed with butyl rubber by melt mixing at different ratios (i.e., 3, 7, 11, and 15 phr). X-ray diffraction results showed that an increase in the amount of organoclay decreased the degree of intercalation. The addition of clay enhanced the physicomechanical properties, including hardness, modulus of elasticity, tensile strength, and elongation at break, in the vulcanized state of all of the nanocomposites.

Peila et al.[13] studied the UV curing of bisphenol A ethoxylate dimethacrylate in the presence of organically modified 5 mol % Cloisite 30B and 5 mol % Cloisite Na^+. DSC analysis evidenced that the T_g values of the nanocomposites did not change with respect to the neat UV-cured resin in the presence of 5 mol % nanofillers. Thermogravimetric analysis in air showed a slight increase in the initial thermal degradation temperatures of the nanocomposites.

In previous investigations, 3 wt % of different clay nanoparticles were incorporated into 2,2-bis[4-(4-maleimidophenoxy phenyl)]propane [bismaleimide (BMIX)]. Both the curing of the BMIX–clay blends and the thermal stability of the cured BMIX–clay nanocomposites have been studied. It has been clearly observed that the presence of Cloisite 15a in BMIX reduces the curing window and imparts excellent thermal stability to the cured nanocomposite.[14] Hence, in this investigation, we intended to investigate in detail the effect of different levels of Cloisite 15a loading in BMIX on the thermal curing behavior with DSC. From the literature survey, it was obvious that nanoparticles have generally been added to a level of 5%, the properties were investigated, and the results were attributed to the intercalation or exfoliation resulting in the medium. There were studies wherein heavy loadings of clay (10, 20, and up to 50%) were added to the polymer matrix, and the effect of loading on the different properties were investigated.[15–22] In this investigation, we investigated the effect of the loading of clay particles (1–9%) on the melting and curing properties of BMIX. The kinetic parameters were calculated with the Flynn–Wall–Ozawa (FWO), Vyazovkin (VYZ), and Friedman (FRD) methods, and the results are discussed.

EXPERIMENTAL

Materials (Laboratory Reagent Grade)

Bisphenol A was purchased from SISCO Research Laboratory Pvt., Ltd. (Mumbai, India). Maleic anhydride, *p*-chloronitrobenzene, and anhydrous sodium acetate were supplied by S. D. Fine-Chem, Ltd. (Mumbai, India). The solvents *N,N′*-dimethyl formamide and acetone were purchased from Merck Specialist Pvt., Ltd. (Mumbai, India). Palladium 10% on carbon was supplied by Lancaster Clariant Group Co. (Chennai, India). Anhydrous potassium carbonate was obtained from RanBaxy Laboratories, Ltd. (New Delhi). Ethyl alcohol and hydrazine hydrate were purchased from Loba Chemie Pvt., Ltd. (Mumbai, India). All of the chemicals were used as received.

Preparation of 2,2-Bis(4-nitrophenoxy phenyl)propane (DN-BPAPCNB)

Bisphenol A (22.8 g), *p*-chloronitrobenzene (34.6 g), and anhydrous potassium carbonate (30.4 g) were placed in a three-necked round-bottom flask containing 125 mL of *N,N′*-dimethylformamide. The reaction mixture showed a color transition from orange to blood red within a few minutes, and potassium chloride precipitated. The resulting reaction mixture was refluxed for 12 h, and the precipitated potassium chloride was filtered off. The filtrate was poured into copious amounts of crushed ice with effective stirring. The separated yellow DN-BPAPCNB was filtered, washed with ice-cold water, and dried at 50°C for 24 h in a hot-air oven. The yield was found to be 90%.

Preparation of 2,2-Bis(4-aminophenoxy phenyl)propane (DA-BPAPCNB)

The dinitro compound (DN-BPAPCNB; 28.2 g) and 0.15 g of 10% Pd/C dispersed in 180 mL of ethanol were placed in a round-bottom flask. Hydrazine hydrate (60 mL) was added

dropwise, and the resulting reaction mixture was refluxed at 85°C for 12.5 h. The hot black solution was filtered to remove palladized charcoal. The filtrate was poured into large amounts of ice-cold water with efficient stirring. A pale gray precipitate of 2,2-bis(4-aminophenoxy phenyl)propane, DA-BPAPCNB was filtered, washed with ice-cold water, and dried at room temperature. The yield of the diamino compound was 85%.

Preparation of Bisamic Acid (BAA)

Exactly 12.3 g of diamine (DA-BPAPCNB) was dissolved in 155 mL of acetone with constant stirring at room temperature. To this solution, 6.5 g of powdered maleic anhydride was added in portions. A yellow precipitate was formed, and it was stirred continuously for 0.5 h. It was filtered and washed with ice-cold acetone to remove acetone-soluble materials and dried. The yield was 86%.

Preparation of BMIX

The yellow BAA was dispersed in a 500-mL, round-bottom flask containing 160 mL of dry acetone. Anhydrous sodium acetate (3.44 g) and acetic anhydride (40 mL) were added to the reaction mixture and refluxed for 3 h. The brown solution was poured into copious amounts of crushed ice, and BMIX (Scheme 1) was obtained as a yellow precipitate. The material was filtered, washed with ice-cold water, and dried *in vacuo*.[14,23] The yield was 90%.

Blending of Organoclay with BMIX

The organoclay Cloisite 15a was dried at 110°C for 24 h in a hot-air oven. The dry Cloisite 15a clay was mixed with BMIX at different weight ratios (1, 2, 3, 4, 5, 7, and 9%) with minimum quantities of acetone. The materials were sonicated for 6 h, then acetone was evaporated, and the dry-blended materials were stored in a desiccator for further analysis.

Methods

The Fourier transform infrared (FTIR) spectra of the blended materials were recorded with a Shimadzu FTIR spectrophotometer 8400S (Kyoto, Japan) with a KBr disc technique. The DSC curves for the blended materials were recorded on a TA Instruments DSC Q10 (Vienna, Austria). The materials were heated from ambient temperature to 400°C at different heating rates (β = 5, 10, 20, and 30°C/min) in a nitrogen atmosphere. SEM images of the thermally cured BMIX and its Cloisite 15a nanocomposite were obtained with a Hitachi S34WON scanning electron microscope.

Kinetic Analysis

If the curing process occurs only by the thermal method, the reaction rate ($d\alpha/dT$) can be obtained by division of the peak height (dH/dT) at temperature T by the total enthalpy of the curing reaction,[24] that is

$$d\alpha/dT = (dH/dT)/\Delta H_c \quad (1)$$

where ΔH_c is the total enthalpy of curing. The fractional conversion (α) can be obtained by the measurement of the partial area of the curing peak:

$$\alpha = \Delta H_T/\Delta H_c \quad (2)$$

where ΔH_T is the enthalpy of the area of the curing peak at a particular temperature.

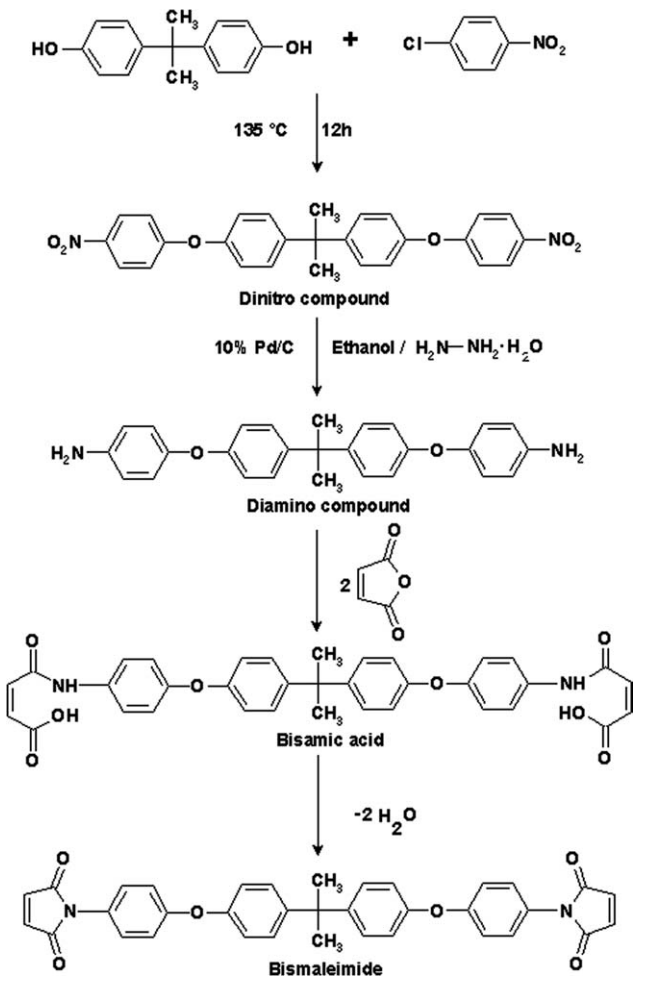

Scheme 1. Preparation of BMIX.

FWO Method

The FWO method is widely used for dynamic kinetic analysis and does not require any assumptions to be made about the conversion-dependence.[25] The equation used for this method is given as follows:

$$E_a = \frac{-R}{1.052}\frac{\Delta \ln \beta}{\Delta\left({}^{1}/_{T}\right)} \quad (3)$$

where R is the gas constant. In this method, plots of ln β versus $1/T$ give parallel lines for each α value. The slope of these lines gives E_a, as per the following expression:

$$\text{Slope} = -0.4567(E_a/R) \quad (4)$$

FRD Method

This is one of the differential methods used to calculate E_a, and the equation is given as follows:[26]

$$\ln\left(\tfrac{d\alpha}{dt}\right) = \ln z + n\ln(1-\alpha) - \left(\tfrac{E_a}{RT}\right) \quad (5)$$

From the slope ($-E_a/R$) of the linear plot between ln($d\alpha/dt$) versus $1/T$, where z is constant, E_a of the system can be calculated.

Applied Polymer SCIENCE

VYZ Method

The integral form of the Arrhenius equation is given as follows:

$$g(\alpha) = \int_0^{\alpha} \frac{d\alpha}{f(\alpha)} = A \int_0^{t} \exp\left(\frac{-E_a(\alpha)}{RT}\right) dt = AJ[E_a(\alpha), T] \quad (6)$$

where $g(\alpha)$ is the integral form of the reaction model $f(\alpha)$, $T(t)$ is the heating program, and A is the Arrhenius constant. With a linear β of dT/dt, $T(t)$ where t is the time, is linear, and in eq. (6), dt can be substituted by dT/β:

$$g(\alpha) = \int_0^{\alpha} \frac{d\alpha}{f(\alpha)} = \frac{A}{\beta} \int_0^{t} \exp\left(\frac{-E_a(\alpha)}{RT}\right) dt = AI[E_a(\alpha), T] \quad (7)$$

Many authors have made numerical approximations to solve the temperature integrals (I and J), and the results of model free kinetics analysis differ widely by the choice of numerical approximations.[27–32] To avoid this dependence on numerical approximation, VYZ and Dollimore used the fact that for any β, $g(\alpha)$ is constant. Thus, with the heating rates β_1, β_2, and β_3, three integrals are obtained, $g(\alpha)_{\beta 1} = g(\alpha)_{\beta 2} = g(\alpha)_{\beta 3}$:

$$\frac{A}{\beta_1} I\left[E_a(\alpha), T\right]_1 = \frac{A}{\beta_2} I[E_a(\alpha), T]_2 = \frac{A}{\beta_3} I\left[E_a(\alpha), T\right]_3$$

Consequently, A can be truncated, and six equations can be formulated:[33]

$$\frac{I[E_a(\alpha),T]_1\beta_2}{I[E_a(\alpha),T]_2\beta_1} = 1 \quad (8)$$

$$\frac{I[E_a(\alpha),T]_2\beta_1}{I[E_a(\alpha),T]_1\beta_2} = 1 \quad (9)$$

$$\frac{I[E_a(\alpha),T]_1\beta_3}{I[E_a(\alpha),T]_3\beta_1} = 1 \quad (10)$$

$$\frac{I[E_a(\alpha),T]_3\beta_1}{I[E_a(\alpha),T]_1\beta_3} = 1 \quad (11)$$

$$\frac{I[E_a(\alpha),T]_2\beta_3}{I[E_a(\alpha),T]_3\beta_2} = 1 \quad (12)$$

$$\frac{I[E_a(\alpha),T]_3\beta_2}{I[E_a(\alpha),T]_2\beta_3} = 1 \quad (13)$$

The summarized equation for the previous is given as follows:

$$\sum_{i=1}^{n} \sum_{j\neq 1}^{n} \frac{I[E_a(\alpha),T]_i\beta_j}{I[E_a(\alpha\alpha),T]_j\beta_i} = 6 \text{ for } n = 3 \quad (14)$$

From the previous equation, the E_a values for the systems can be calculated.

RESULTS AND DISCUSSION

FTIR Studies

The FTIR spectra of BMIX, Cloisite 15a, and its blends are shown in Figure 1. The presence of the bands corresponding to —C—O—C— stretching (1149 cm^{-1}), C=C stretching for a phenyl nucleus (1396 cm^{-1}), C=C stretching for imide ring (1635 cm^{-1}), and cyclic imide —OC—N—CO— stretching (1712 cm^{-1}) in the FTIR spectrum of BMIX confirmed its structure.

The bands at 1149 and 1396 cm^{-1} in the BMIX–clay blends showed no sign of any change. This revealed that the clay particles did not interact with the bisphenol part present in BMIX.

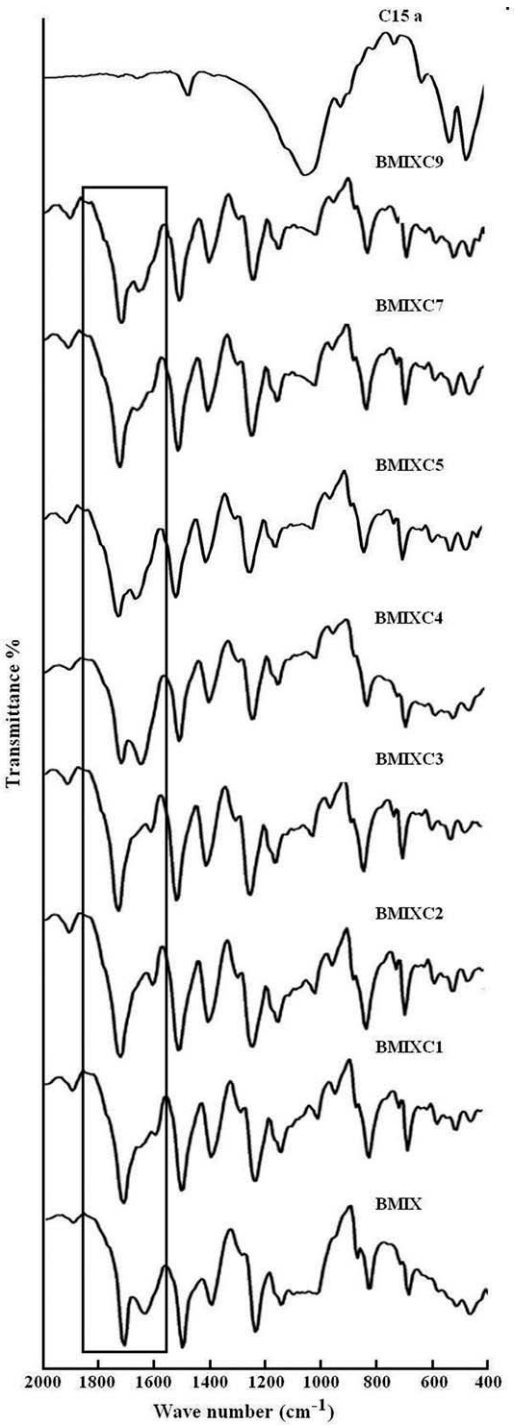

Figure 1. FTIR spectra of BMIX and its Cloisite 15a (C15a) nanoclay blends.

The band at 1010 cm^{-1} in all of the blends was attributed to the Cloisite 15a clay. At 1% clay loading in BMIX, the band at 1635 cm^{-1} disappeared and showed a little absorption at 1597 cm^{-1}. This absorption was a little stronger at 2 and 3% clay loadings in the BMIX matrix. At 4 and 5% clay loadings, a band at 1643 cm^{-1}, overlapping with the cyclic imide ring band, was noted. When the clay loadings were 7 and 9%, a peak at a slightly higher frequency (1713 cm^{-1}) was noted, and

there was no interaction with the cyclic imide ring band. In blends where the clay loading was less, some sort of weak interaction was expected between the clay platelets and the maleimide part of the BMIX molecule. As the clay loading increased, this interaction was stronger because of the availability of the clay platelets.

DSC studies

The DSC curves recorded at $\beta = 5°C/min$ for BMIX and its blends with Cloisite 15a and the DSC curves for BMIX at multiple β's (5, 10, 20, and 30°C/min) are shown in Figures 2 and 3, respectively. The values obtained for the parameters such as melting temperature (T_m), enthalpy of fusion (ΔH_f) and ΔH_c from the DSC traces at different β values for BMIX and its blends with Cloisite 15a are tabulated in Table I. The detailed observations from the DSC traces recorded at $\beta = 10°C/min$ are discussed later. BMIX showed a sharp T_m at 83°C, and the enthalpy of fusion was 8.4 J/g. The onset of curing was noted around 189°C; curing attained a maximum at 277°C and ended at 362°C. The value of ΔH_c was 157 J/g, and the temperature region of the curing window was 173°C. There was no characteristic change in the T_m of BMIX up to a 5% loading of clay, and the T_m values decreased to 61 and 59°C at Cloisite 15a loadings of 7 and 9%, respectively, in the BMIX. The incorporation of Cloisite 15a in BMIX affected the sharp melting behavior of BMIX and broadened the melting peak. Higher loadings of Cloisite 15a in BMIX further decreased the intensity of melting, and only a small melting peak was observed. This observation clearly indicated that interactions existed between the BMIX molecules and the Cloisite 15a clay particles. The enthalpy of fusion of the pure BMIX (8.4 J/g) gradually decreased up to 5% loading of the clay particles and decreased in appreciable quantities for 7 and 9% clay loadings in the BMIX system. The change that was observed in the melting region and the drastic difference noted in the ΔH_f values for the pure BMIX and the BMIX/Cloisite 15a blends provided very good evidence

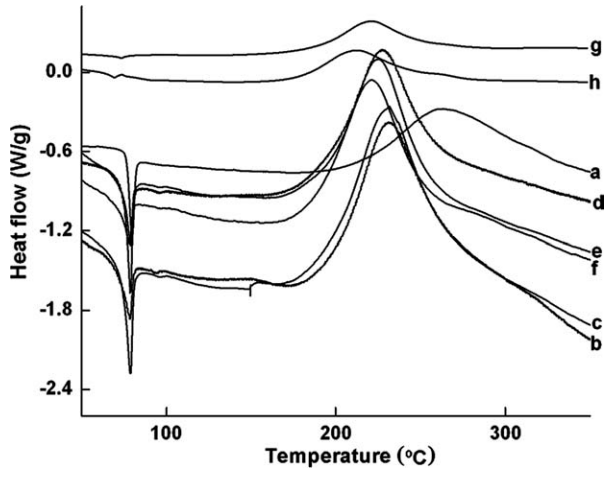

Figure 2. DSC traces of BMIX and its Cloisite 15a blends at $\beta = 5°C/min$: (a) BMIX, (b) BMIX + 1% Cloisite 15a, (c) BMIX + 2% Cloisite 15a, (d) BMIX + 3% Cloisite 15a, (e) BMIX + 4% Cloisite 15a, (f) BMIX + 5% Cloisite 15a, (g) BMIX + 7% Cloisite 15a, and (h) BMIX + 9% Cloisite 15a.

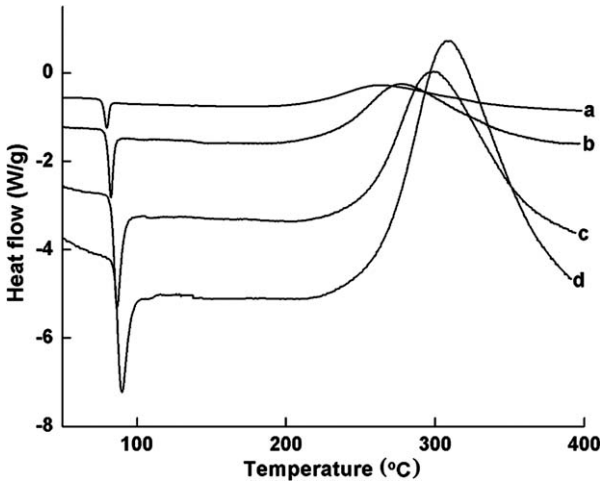

Figure 3. DSC traces of BMIX at different β's: (a) 5, (b) 10, (c) 20, and (d) 30°C/min.

for the interactions existed between BMIX and Cloisite 15a clay at room temperature. The intensity of this interaction differed with the amount of nanoclay in the BMIX system.

Ersali et al.[12] studied the physical properties of ethylene–propylene–diene monomer/acrylonitrile butadiene rubber/organoclay nanocomposites and observed that the addition of organoclays reduced the curing time. They concluded that it may have been because of the formation of complexes between quaternary amine groups in the organoclay and zinc salt or sulfur, which accelerated the curing process. It was observed that the presence of higher quantities of nanoclay in the rubber matrix led to a higher crosslinking density during curing.

The shape of the curing curves of the BMIX/Cloisite 15a blends were similar to the shape of the curing curve recorded for BMIX. Hao et al.[34] investigated the curing behavior of industrial-grade bisphenol A based epoxide and its composites with polyhedral oligomeric silsesquioxane with DSC and observed the presence of a single exothermic peak in all cases; this indicated the homogeneous mixing of nanoparticles in the epoxy matrix. On the basis of the previous study, it is reasonable to state that there was homogeneous mixing in this system of BMIX/Cloisite 15a nanoclay blends. From Table I, it is evident that the introduction of Cloisite 15a nanoclay particles in BMIX decreased the curing onset temperature by around 20°C up to a clay loading of 5%. The further addition of Cloisite 15a in BMIX still reduced the curing exotherm onset by 35 and 25°C when the loadings of nanoclay were around 7 and 9%, respectively. The curing maximum was noted around 277°C for pure BMIX when it was heated at a β of 10°C/min. The incorporation of nanoclay in BMIX shifted this curing exotherm to approximately 240°C; this was around 40°C less than the pure BMIX. The polymerization reaction, because of the olefinic bond present in the maleimide part of BMIX, which led to crosslinking, was definitely influenced by the presence of Cloisite 15a nanoclay particles in the molten BMIX matrix. The interactions, which were evidenced by the variations in T_m and ΔH_f noted in the BMIX and BMIX/Cloisite 15a nanoclay blends at ambient, were maintained in the dispersion of the clay

Table I. DSC Studies of BMIX and Its Cloisite 15a Blends at Different β values

Sample	β (°C/min)	T_m (°C)	ΔH_f (J/g)	Onset T_S (°C)	Endset T_E (°C)	$T_E - T_S$ (°C)	Maximum (°C)	ΔH_c (J/g)
BMIX	5	80	8.1	187	360	173	263	144.3
	10	83	8.4	189	362	173	277	157.1
	20	87	8.9	204	390	186	301	155.2
	30	89	7.4	217	390	173	307	142.8
BMIX + 1% Cloisite 15A	5	78	5.0	171	298	127	231	105.0
	10	81	6.1	185	340	155	245	125.3
	20	84	6.0	196	348	152	259	125.2
	30	86	6.6	194	383	189	270	128.6
BMIX + 2% Cloisite 15A	5	79	7.2	167	294	127	229	105.1
	10	82	7.1	171	334	149	241	108.9
	20	84	9.8	189	375	186	255	111.5
	30	87	10.7	202	367	165	265	112.7
BMIX + 3% Cloisite 15A	5	79	7.9	160	317	157	227	109.6
	10	82	8.2	175	321	146	239	104.1
	20	85	6.9	181	348	167	254	110.1
	30	87	14.2	190	373	183	263	107.4
BMIX + 4% Cloisite 15A	5	79	5.3	163	285	122	225	101.7
	10	81	6.4	169	317	148	235	104.3
	20	84	9.0	179	346	167	250	115.3
	30	86	4.3	189	342	153	258	116.0
BMIX + 5% Cloisite 15A	5	78	5.1	161	300	139	221	104.4
	10	81	6.0	175	308	133	237	108.2
	20	84	7.0	187	333	146	251	119.9
	30	87	5.6	179	350	171	261	124.8
BMIX + 7% Cloisite 15A	5	74	1.2	163	288	125	221	121.1
	10	61	0.4	155	300	145	226	126.5
	20	79	2.2	193	294	101	245	113.1
	30	79	3.4	173	307	134	253	131.0
BMIX + 9% Cloisite 15A	5	69	1.6	168	286	118	212	128.8
	10	59	1.0	165	294	129	224	144.1
	20	75	4.3	184	296	112	236	148.1
	30	79	3.3	181	306	125	248	139.8

particles in the molten BMIX matrix. All of the blends showed curing maximum temperatures at around 225–245°C.

From Table I, the DSC parameters for BMIX and its blends recorded at 5°C/min clearly showed that the incorporation of Cloisite 15a nanoparticles led to a decrease in the onset temperature of BMIX from 187 to around 165°C, that is, a decrease of around 20°C, and the maximum temperature value decreased from 263 to around 230°C, that is, a decrease of around 30°C. However, the temperature at which curing was nearly complete decreased from 360 to around 290°C, that is, a decrease of around 70°C. If the interaction and/or the influence exercised by the clay particles on the BMIX molecules were uniform right from the beginning of polymerization until the end of the curing reaction, uniform shifts of temperature at curing starts (T_S), temperature at curing ends (T_E), and temperature at maximum curing (T_{max}) were expected. Deviations from this observation in this system indicated clearly that the Cloisite 15a nanoparticles affected the polymerization or the crosslinking reactions of BMIX in a nonuniform fashion. The same arguments could be extended to nearly all of the clay loadings in BMIX and also to the systems investigated at different β values. ΔH_c decreased by 30, 50, and 10 J/g for 1, 2–5, and 7–9% loadings, respectively, of Cloisite 15a in BMIX. The FTIR studies indicated the existence of interactions between the olefinic bond present in the cyclic imide part of BMIX and the Cloisite 15a nanoclay. Hence, it was reasonable to expect variations in the curing parameters of the BMIX–Cloisite 15a nanoclay blends. As to the expectations, the parameters obtained from the DSC studies revealed the influence shown by the presence of nanoclay particles in the BMIX matrix.

Lee and Han[7] studied the interaction between Cloisite 30B nanoclay and a polystyrene-*block*-hydroxylated polyisoprene

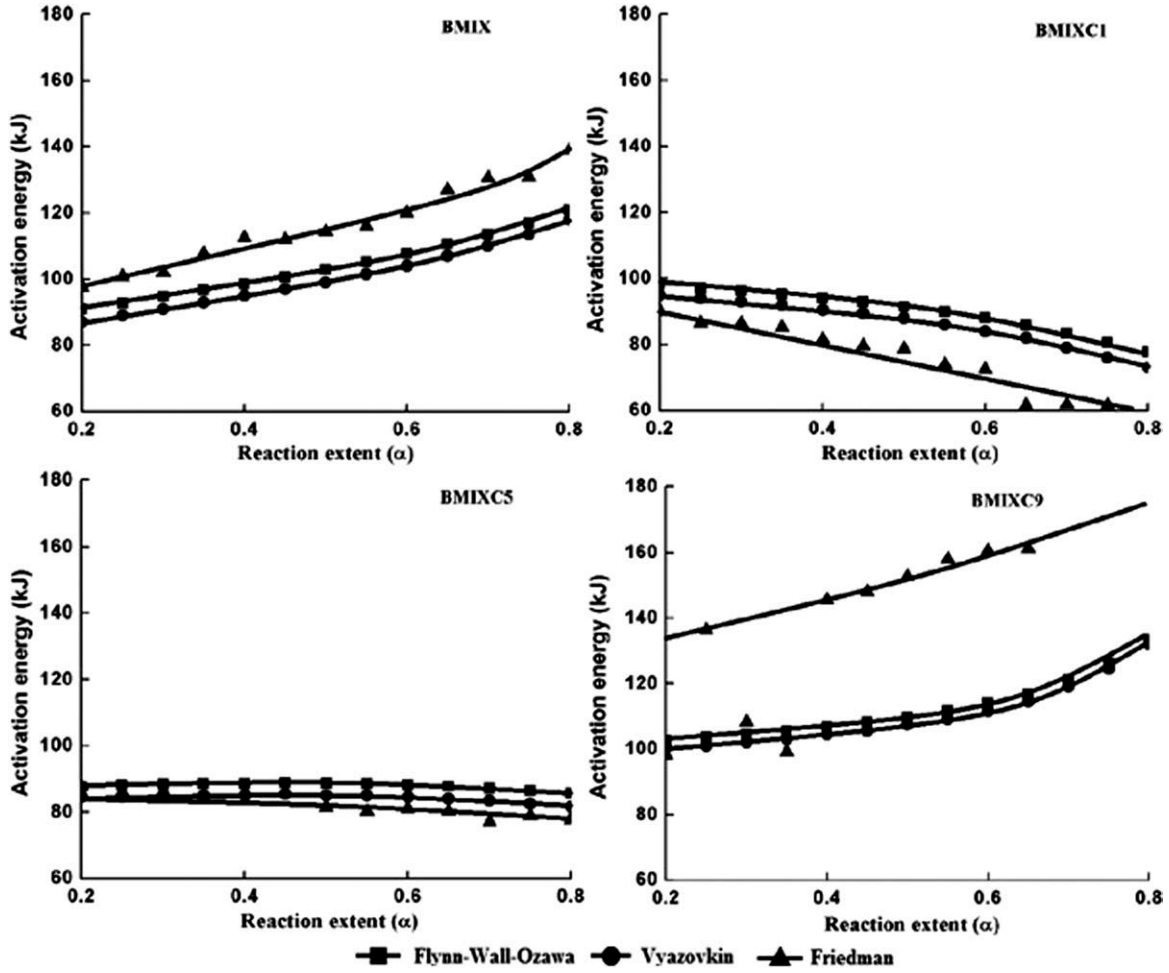

Figure 4. Relative reaction extent versus E_a of BMIX and its Cloisite 15a nanoclay blends.

copolymer. During the mixture of clay particles into the polymer matrix, the hydroxyl groups present in the copolymer formed hydrogen bonds with the polar groups of the organoclay particles and facilitated higher degrees of exfoliation of organoclay aggregates. Likewise, in this system, the olefinic link may have interacted efficiently with the clay particles.

Kinetic Studies

Three different kinetic methods (FWO,[25] VYZ,[33] and FRD[26]) were used for the kinetic study of the curing of BMIX and its blends. The plots between E_a and the reaction extent (α) values of BMIX, BMIXC1, BMIXC5, and BMIXC9 obtained for the thermal curing of these materials with the mentioned kinetic methods are shown in Figure 4, and the values for all of the materials investigated are tabulated in Table II. The plots between E_a and the reaction extent (α) values for all of the materials by the FWO method are shown in Figure 5.

The E_a values calculated by these three methods agreed very well, and the trends in the variation of E_a for the curing of the different materials investigated were nearly the same. The apparent E_a values calculated for the curing of BMIX and its Cloisite blends by the FWO and VYZ methods were the same, but the values obtained by the FRD method differed from those obtained by the other two methods. This was because of the way in which E_a was calculated; that is, the kissinger akahira sunose (KAS) and FWO methods are integral methods, and FRD is a differential method. Jankovic et al.[35] studied the kinetics of the nonisothermal dehydration of equilibrium swollen poly(acrylic acid) hydrogels with thermogravimetric analysis by five different isoconversional methods [FRD, FWO, KAS, Tang (T), and VYZ]. The change in E_a with respect to the reaction extent for the methods FWO, KAS, T, and VYZ led to close values of E_a, but these values differed substantially from the values of E_a obtained with the isoconversional method suggested by FRD. The authors suggested that these differences could have been due to the approximation of the relations that grounded the FWO, KAS, T, and VYZ methods, and the differences between the apparent E_a's calculated with the FRD method and the values of E_a calculated with the other isoconversional methods were due to the way in which the relations that formed the basis of the integral methods were derived.

The E_a value for BMIX was observed to increase gradually with increasing extent of reaction (α). Generally, in the curing process or the curing reactions of thermoset resins, molecules undergo gelation (from liquid to rubber) and, finally, vitrification (from rubber to glass) transitions. The crosslinking process

Table II. E_a Values for the Thermal Curing of BMIX and Its Cloisite 15a Nanoclay Blends

		α and E_a values												
Sample	α	0.2	0.25	0.3	0.35	0.4	0.45	0.5	0.55	0.6	0.65	0.7	0.75	0.8
BMIX	FWO	91	93	95	97	99	101	103	105	108	111	114	117	121
	VZY	87	89	91	93	95	97	99	102	104	107	110	114	118
	FRD	98	101	102	108	113	112	114	116	120	127	131	131	139
BMIX + 1% Cloisite 15A	FWO	98	97	96	95	94	93	92	90	88	86	83	81	78
	VZY	95	94	93	92	91	90	88	86	84	82	79	76	73
	FRD	90	86	86	85	82	80	79	74	72	62	62	61	58
BMIX + 2% Cloisite 15A	FWO	101	101	100	100	99	98	97	95	93	90	88	84	79
	VZY	99	98	98	97	96	95	94	92	90	87	84	80	75
	FRD	97	94	93	91	86	87	80	78	74	66	65	58	55
BMIX + 3% Cloisite 15A	FWO	100	100	100	100	99	98	97	96	95	93	91	89	86
	VZY	98	98	97	97	96	95	94	93	91	90	87	85	82
	FRD	99	97	96	93	93	89	85	81	80	80	73	74	72
BMIX + 4% Cloisite 15A	FWO	105	105	105	104	104	103	102	101	100	98	96	93	90
	VZY	103	103	102	102	101	100	99	98	97	95	93	90	86
	FRD	103	96	100	98	97	103	98	91	84	79	73	70	65
BMIX + 5% Cloisite 15A	FWO	88	88	88	89	89	89	89	89	88	88	87	86	86
	VZY	85	85	85	85	85	86	85	85	85	84	84	83	82
	FRD	88	86	86	84	86	86	81	80	81	80	77	79	78
BMIX + 7% Cloisite 15A	FWO	102	103	105	107	108	110	112	114	116	119	123	129	136
	VZY	99	101	103	104	106	108	110	112	114	118	121	127	134
	FRD	105	111	128	110	103	106	117	112	118	133	141	145	156
BMIX + 9% Cloisite 15A	FWO	103	104	105	106	107	108	110	112	114	117	121	126	133
	VZY	101	101	102	103	105	106	108	109	112	115	119	125	132
	FRD	98	136	108	99	146	148	153	158	161	161	180	191	156

reduces the molecular mobility and results in a change from a kinetically controlled to a diffusion-controlled reaction during the curing of thermosetting resins.[36,37]

The following recommendation was developed by the Kinetics Committee of the International Confederation for Thermal Analysis and Calorimetry:[38] because the relative experimental errors in the kinetic data are larger at the lowest and highest conversions, it might be advisable to limit analysis to certain ranges. After, a reaction extent value of 0.8, vitrification is caused in thermoset matrix systems by a shift from a kinetic to a diffusion-control reaction. Hill et al.[39] studied the kinetics and curing mechanism of a BMIX–diamine thermoset matrix systems. They explained that an excellent fit to the experimental data for the consumption of primary and secondary amines was obtained with the kinetic rate laws up to approximately 70% conversion. At higher conversions, a negative deviation from the predicted rates was found. This was attributed to vitrification, which led to an element of diffusion control in the reaction. The effect of diffusion control could be accounted for by the inclusion in the kinetic equation a term related to the T_g of the network and an E_a for segmental motion. So, in this system, we calculated E_a's for the reaction extent values of 0.2–0.8.

In this system, E_a calculated by the FWO method for the BMIX polymerization increased from 91 to 121 kJ/mol as the extent of the reaction (α) value increased from 0.2 to 0.8. Up to a reaction extent of 0.6, E_a increased slowly afterward. The rate of increase in the E_a value was different. Initially, the concentration of the monomer (BMIX) was high, and hence, the polymerization reaction was easier and involved low-energy requirements. As the reaction proceeded, the availability of the monomer decreased, and the viscosity of the polymerizing medium increased. This increasing viscosity and the dearth in the

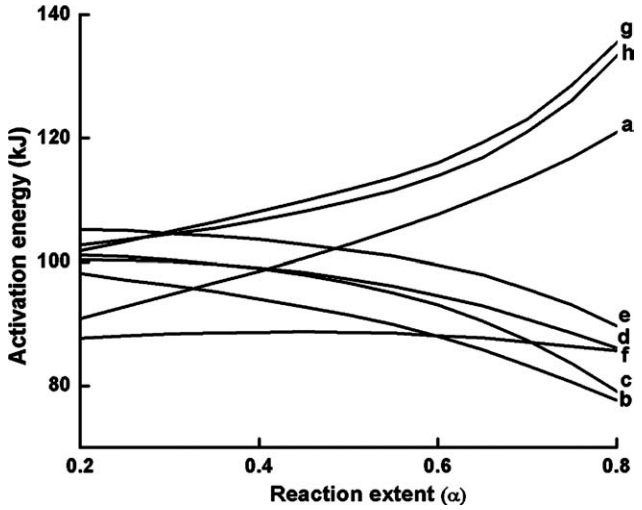

Figure 5. Relative reaction extent versus E_a of BMIX and its Cloisite 15a nanoclay blends as determined by the FWO method: (a) BMIX, (b) BMIX + 1% Cloisite 15a, (c) BMIX + 2% Cloisite 15a, (d) BMIX + 3% Cloisite 15a, (e) BMIX + 4% Cloisite 15a, (f) BMIX + 5% Cloisite 15a, (g) BMIX + 7% Cloisite 15a, and (h) BMIX + 9% Cloisite 15a.

polymerizable groups made the crosslinking reaction difficult. So at this stage, the system needed a higher energy for polymerization; that is, E_a gradually increased. As the extent of the polymerization neared completion, the viscosity of the medium was sufficiently high, and the availability of monomer and polymerizable groups was much lower. So, E_a was comparatively higher for the final stages of polymerization.[34,40] The possible polymerization of BMIX is shown in Scheme 2.

He et al.[41] studied the curing kinetics of phenol formaldehyde resin systems and observed a fast increase in E_a at low conversion extents. Because the reaction was almost complete and because of the lower availability of the reactive groups, the addition reactions were few, and hence, at low conversion, E_a increased. The rapid decrease of E_a at high conversion extents could be explained by the change in the reaction mechanism from kinetically controlled to diffusion controlled.

Mija et al.[42] studied the kinetics of the acid-catalyzed curing of furfuryl alcohol with model-free kinetics. The different apparent E_a values obtained for the different conversions led to the conclusion that the nonisothermal acid-catalyzed polymerization followed multistep kinetics. The decrease in the E_a values when α was lower than 0.1 was explained by a diffusion-controlled kinetics due to the high viscosity of the medium. For $0.1 < \alpha < 0.4$, the E_a values were around 60 kJ/mol with a quasi-constant conversion. This suggested that a single reaction dominated in this conversion range. For $0.63 < \alpha < 0.85$, E_a of the system increased. As the temperature increased linearly in the nonisothermal experiments, the chain mobility increased, and the chemical reactions were reactivated. In the later stages of the reaction, the rate of crosslinking was limited by the mobility of the longer polymer chains, and diffusion encountered a large energy barrier because of the cooperative nature of the motions. This led to higher E_a values. At higher α values, the E_a value decreased. The monomer molecules became frozen in their positions in the glassy state, and this resulted in a virtual cessation of the reaction. The curing rate in the glassy state became controlled by the diffusion of small, unreacted functions still present in the medium, and the chemical reactions were considerably reduced. This meant that vitrification caused a dramatic decrease in the molecular mobility, which led to a decrease in the effective E_a with increasing extent of reaction.

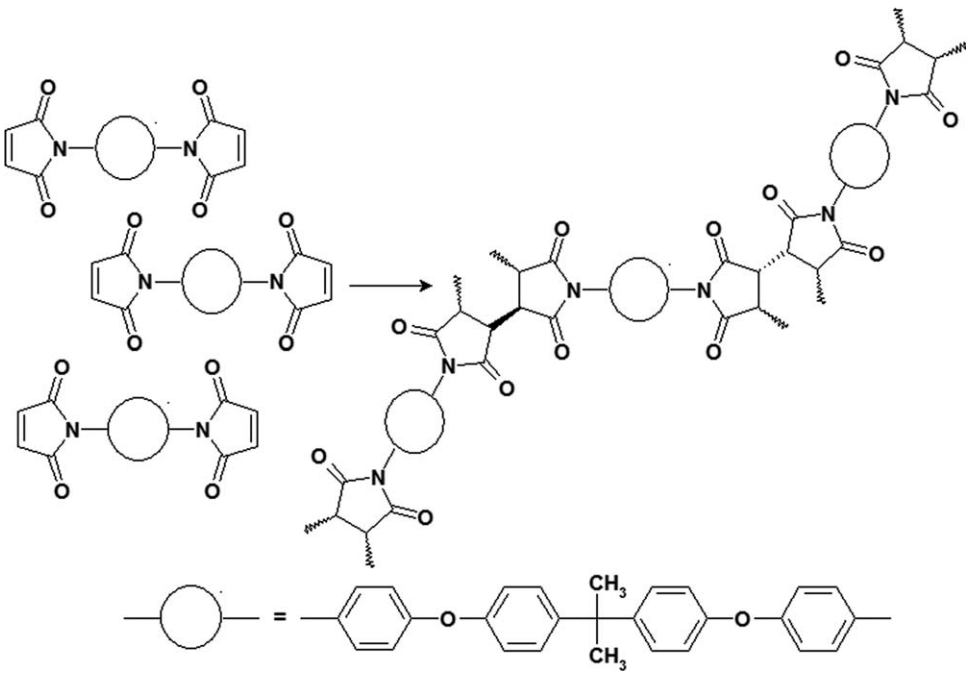

Scheme 2. Polymerization of BMIX.

Applied Polymer SCIENCE

The incorporation of the nanoclay Cloisite 15a in BMIX must have had some influence on the polymerization of BMIX. The E_a curves for the BMIX systems containing 1–4% Cloisite 15a progressively decreased as the reaction extent increased. E_a for the polymerization was initially higher than the pure BMIX, and as the reaction proceeded, E_a decreased. The presence of 5% Cloisite 15a in BMIX showed completely different behavior, wherein the extent of the reaction (α) did not influence the E_a values. Further increases in the loading of nanoparticles (to 7 and 9% Cloisite 15a) in BMIX showed a very similar variation in the E_a values with respect to increases in reaction extent values, but the E_a values were considerably higher than those noted for BMIX and BMIX with low-level Cloisite 15a loadings (1–4%). At higher Cloisite 15a loadings, another interesting observation noted was that when the reaction extent was greater than 0.65, E_a increased very steeply.

Ngo et al.[5] studied the curing kinetics of epoxy nanocomposites. The nanocomposites were prepared with Cloisite 30B (2 and 4 wt %) by direct mixing at room temperature and higher temperatures. In the pure resin system, the E_a values increased steadily with conversion. The E_a curve for the 2 wt % nanoclay mixed with epoxy was similar to that of the virgin monomer, but the values were higher than those of the virgin monomer. The E_a values for the materials (with 2 and 4 wt % Cloisite 30B in epoxy) blended at higher temperature decreased slightly as the degree of conversion increased. The authors concluded that the mixing method affected the E_a value of the epoxy resin.

Cao et al.[36,40] studied the curing kinetics of phenol formaldehyde resin with wood flakes and ammonium pentaborate (APB), a fire retardant. They used five different levels of APB loading, in which 8.88 wt % APB incorporation showed a different trend in the E_a curve. E_a suddenly increased up to 40% conversion and then decreased. The authors concluded that the addition reactions were few and were almost complete at the beginning of the curing process and that the mechanism of curing was a quite different one.

In general, intercalation is observed when the polymer matrix and layered silicates do not have sufficient interactions, whereas exfoliation is observed when a polymer matrix and layered silicates have strong attractive interactions.[7] From FTIR studies, we observed that the clay particles had strong interactions only with the imide ring part of the BMIX and not with the other parts. When the BMIX molecules intercalated into the clay galleries, the whole part of the BMIX molecule interacted with the clay particles. The imide ring of BMIX interacted with both surfaces of the clay platelet clusters; these were already modified with dimethyldihydrogenated tallow quaternary ammonium salt. Because the olefinic link present in the imide ring of BMIX was considerably electron rich, it may have had interactions with the electron-deficient centers present at the surface of the clay particles. In the virgin BMIX system, because of the presence of only BMIX molecules, the approach of the monomer molecules for polymerization was easier at the initial stages of thermal curing. As the polymerization proceeded, the decreasing concentration of monomers and the increasing viscosity of medium having sufficiently crosslinked oligomers increased the E_a necessary for further polymerization.

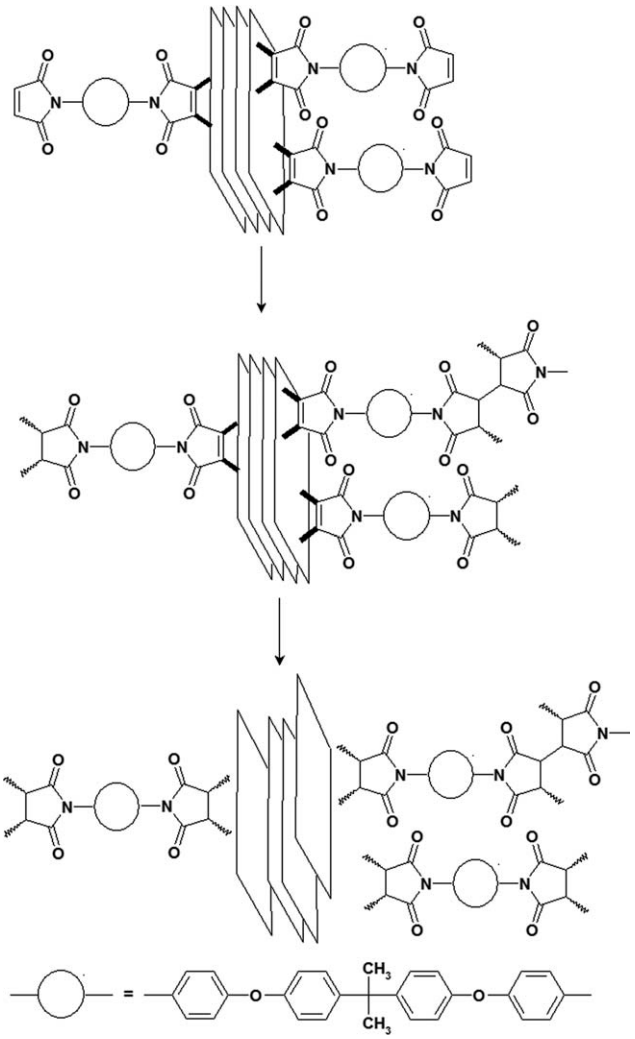

Scheme 3. Polymerization of BMIX at lower loadings of Cloisite 15a (1–4%) nanoclay.

When the Cloisite 15a nanoclay was loaded into BMIX at low concentrations, anchoring of the BMIX molecules on both sides of the clay platelet layers was possible, as shown in Scheme 3. Compared to that in the pure BMIX, the availability of polymerizable groups was lower in the clay-blended systems. Hence, for all of the clay-loaded systems, except those with a clay loading of 5%, the initial E_a calculated at low levels of reaction extent was higher than that of the pure BMIX system. As the polymerization progressed, systems having low levels of clay (<4%) showed a continuous decrease in E_a. Because the material was continuously heated, the weak attraction that existed between the clay surface and the BMIX molecule decreased; this led to the availability of polymerizable sites. Furthermore, the possibility of the slippage of the clustered platelets of the clay particles in the polymerizing medium decreased the viscosity of the medium and led to a favorable situation for the remaining sites present; hence, E_a decreased. The interplay of these two factors may have been the reason for the decrease in E_a with increasing reaction extent at low levels of Cloisite 15a. The E_a for the materials with low clay loadings (1–4% Cloisite 15a in

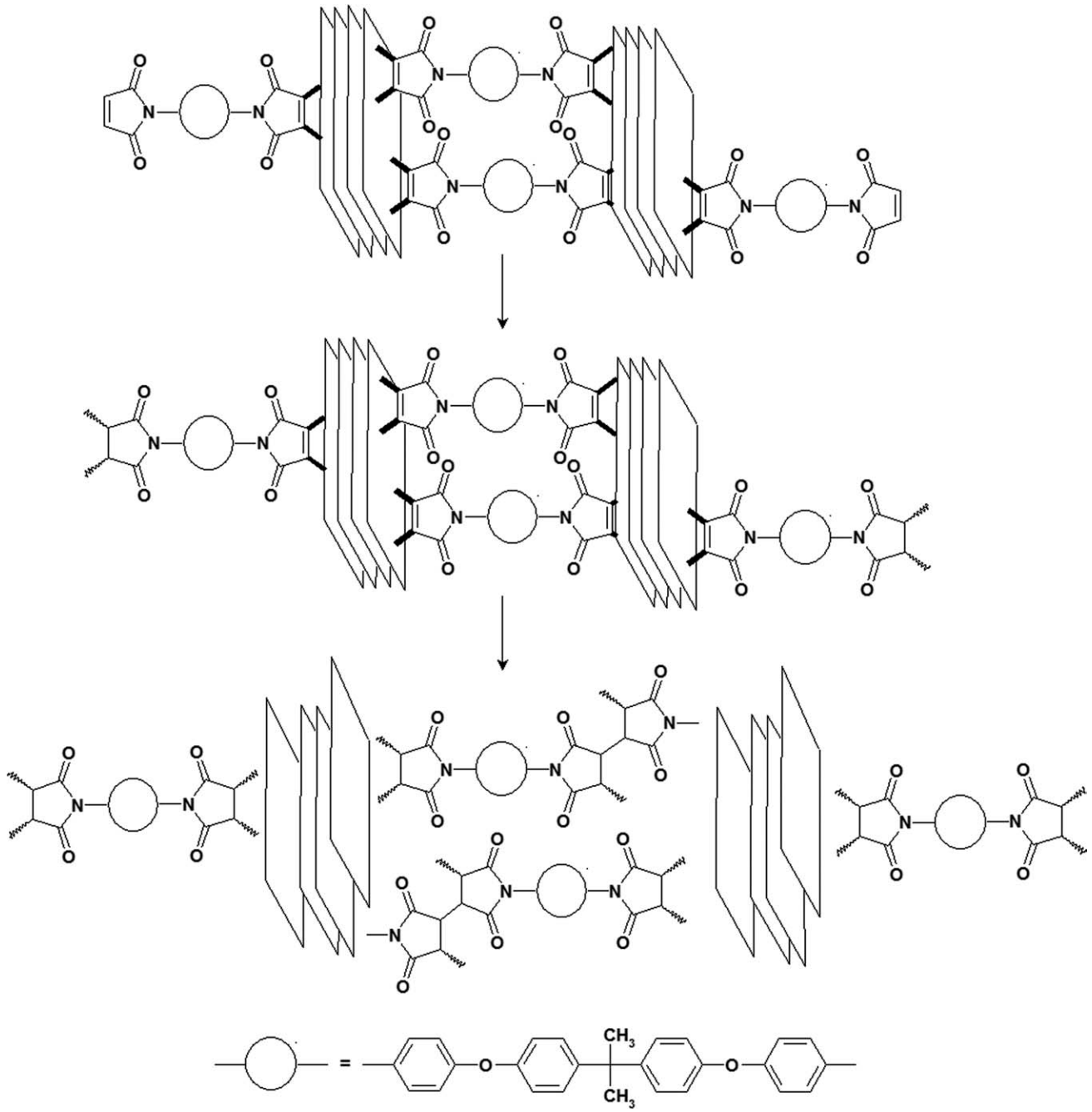

Scheme 4. Polymerization of BMIX at higher loadings of Cloisite 15a (7 and 9%) nanoclay.

BMIX) was 30 kJ/mol lower than BMIX at a reaction extent level of 0.8. At a particular reaction extent, the E_a values for different clay loadings increased as the amount of clay particles incorporated in BMIX increased.

For higher loadings of clay (7 and 9% Cloisite 15a with BMIX), the variation of E_a with respect to the increasing extent of conversion (α) was similar to that in the pure BMIX system, but the E_a values were higher. In the 7 and 9% Cloisite 15a nanoclay loaded systems, because of the presence of more clay particles, the possibility of surface interaction of both of the imide groups present in BMIX with the surface of the clay platelet clusters was sufficiently high (Scheme 4). Hence, E_a for the polymerization was higher. As the polymerization proceeded, the increase in temperature experienced by the system led to a decrease in interaction between the clay surface and the partially polymerized BMIX molecules; this led to the liberation of reactive sites. A restriction of the mobility imposed on the oligomeric materials formed, and the presence of sufficiently higher amounts of clay platelets led to difficulty in the polymerization and was reflected in the increase in E_a.

The 5% Cloisite 15a blended BMIX system behaved in an entirely different manner compared to all of the other systems

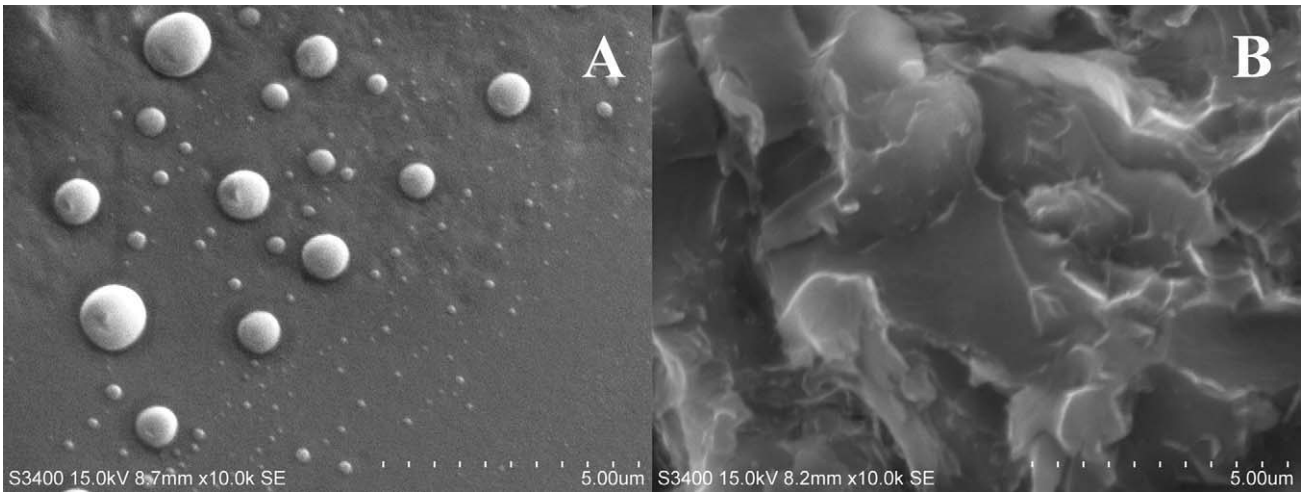

Figure 6. SEM images of the (A) thermally cured BMIX and (B) BMIX + 5% Cloisite 15a.

investigated. From Figure 5, it is very clear that the BMIX system loaded with 5% Cloisite 15a did not show any influence on E_a for the crosslinking reaction with variation in the extent of reaction. The constancy of E_a with respect to an increasing reaction extent value was due to a single reaction that was dominant in this conversion range.[42] In systems with low clay loadings (1–4% Cloisite 15a), the E_a values continuously decreased as the extent of the reaction increased, whereas at higher clay loadings (≥7%), the phenomenon was reversed. One of the possible explanations for the constant E_a for α values of 0.2–0.8 in the case of the 5% Cloisite 15a nanoclay loaded BMIX was the complex interplay of the two opposing factors noted in the materials with low and higher levels of the Cloisite 15a.

SEM Studies

The surface morphologies of the thermally cured BMIX and the nanocomposite of BMIX with 5% Cloisite 15a were studied with SEM, and the SEM images are shown in Figure 6. The SEM image of pure BMIX showed a smooth surface of polymerized BMIX and some voids formed during the polymerization. The image of the nanocomposite of BMIX with 5% Cloisite 15a showed that the nanoclay particles were dispersed almost uniformly throughout the BMIX matrix system.

CONCLUSIONS

BMIX was prepared from BAA by imidization with acetic anhydride. Cloisite 15a nanoclay was incorporated into BMIX systems in different proportions and ultrasonicated. FTIR results reveal that the Cloisite 15a clay had strong interactions with the imide ring of the BMIX, and it did not with the other structural entities of the BMIX. The curing studies of the synthesized materials were performed with DSC, and we found out that the Cloisite 15a nanoclay affected the melting and curing behavior of BMIX. The curing kinetics of the synthesized materials were studied with the FWO, VYZ, and FRD kinetic methods, and the results obtained were similar. As the extent of polymerization in BMIX increased, E_a for curing also increased. The incorporation of 1–4% nanoclay in BMIX gradually increased E_a for curing; this initially indicated that interactions existed between the surface of the clay platelet clusters and the BMIX molecules. As the extent of the reaction increased, E_a for curing gradually decreased; this indicated the loss of interactions, which led to the availability of reactive centers. At higher clay loadings (7 and 9% Cloisite 15a), E_a for curing progressively increased as the extent of the reaction increased; this indicated restricted chain mobility and a low availability of reactive sites. The near constancy noted in the E_a values at various reaction extent values in the 5% Cloisite 15a loaded BMIX indicated an opposing interplay of factors responsible for the variation in E_a values at lower (1–4%) and higher (7 and 9%) clay loading in the BMIX system that we investigated. The surface morphology of the thermally cured BMIX and the nanocomposite of BMIX with 5% Cloisite 15a indicated the good dispersion of clay particles in the cured BMIX matrix system.

ACKNOWLEDGMENTS

The authors thank the Directorate of Extramural Research & Intellectual Property Rights, Defence Research & Development Organization, Ministry of Defence, Government of India, New Delhi, for financially supporting this work under grant ERIP/ER/0704359/M/01/1101, dated December 12, 2008. The authors express their sincere thanks to the Management and Principal of Kamaraj College of Engineering and Technology, India and Thiagarajar College, for providing all of the facilities to do the work.

REFERENCES

1. Shokralahi, F.; Sadi, M.; Shokralahi, P. *J. Therm. Anal. Calorim.* **2005,** *82*, 151.
2. Agnieszka, L.; Krzysztob, P. *J. Therm. Anal. Calorim.* **2008,** *93*, 677.
3. Lee, J. Y.; Choi, B. C.; Lee, H. K. *Adv. Mater. Res.* **2010,** *123*, 667.
4. Vijayakumar, C. T.; Periadurai, T.; Alam, S. *Polym. Plast. Technol.* **2009,** *48*, 141.
5. Ngo, T. D.; Ton-That, M. T.; Cole, K. C.; Hao, S. V. *Compos. Sci. Technol.* **2009,** *69*, 1831.

6. Lee, K. M.; Han, C. D. *Macromolecules* **2003,** *36*, 7165.
7. Lee, K. M.; Han, C. D. *Macromolecules* **2003,** *36*, 804.
8. Southern Clay Products. Cloisite® 15A Typical Physical Properties. Bulletin. http://www.scprod.com/product_bulletins/PB%20Cloisite%2015A.pdf. Accessed on September 15, 2011.
9. Manoratne, C. H.; Rajapakse, R. M. G.; Dissanayake, M. A. K. L. *Int. J. Electrochem Sci.* **2006,** *1*, 32.
10. Razzaghi-Kashani, M.; Hasankhani, H.; Kokabi, M. *Iran Polym. J.* **2007,** *16*, 671.
11. Reddy, M. M.; Gupta, R. K.; Bhattacharya, S. N.; Parthasarthy, R. *Korea Aust. Rheol. J.* **2007,** *19*, 133.
12. Ersali, M.; Fazeli, N.; Naderi, G. In Proceedings of the 6th Nanoscience and Nanotechnology Conference, Izmir, Turkey, June **2010**; p 712. Available at: http://nanotr6.iyte.edu.tr/docs/conference-book/Poster%20Presentations-3rdDay.pdf. Accessed on September 15, 2011.
13. Peila, R.; Malucelli, G.; Priola, A. *J. Therm. Anal. Calorim.* **2009,** *97*, 839.
14. Vijayakumar, C. T.; Surender, R.; Rajakumar, K.; Alam, S. *J. Therm. Anal. Calorim.* **2010,** *103*, 693.
15. Sanchez-Soto, M.; Schiraldi, D. A.; Illescas, S. *Eur. Polym. J.* **2009,** *45*, 341.
16. Ramirez, C.; Rico, M.; Torres, A.; Barral, L.; Lopez, J.; Montero, B. *Eur. Polym. J.* **2008,** *44*, 3035.
17. Ghaemy, M.; Bazzar, M.; Mighani, H. *Chin. J. Polym. Sci.* **2011,** *29*, 141.
18. Erdoan, B. C.; Seyhan, A. T.; Ocak, Y.; Tanolu, M.; Balkose, D.; Ulku1 S. *J. Therm. Anal. Calorim.* **2008,** *94*, 743.
19. Perez, C. J.; Alvarez, V. A.; Stefani, P. M.; Vazquez, A. *J. Therm. Anal. Calorim.* **2007,** *88*, 825.
20. Olewnik, E.; Garman, K.; Ski, W. C. *J. Therm. Anal. Calorim.* **2010,** *101*, 323.
21. Causin, V.; Marega, C.; Saini, R.; Marigo, A.; Ferrara, G. *J. Therm. Anal. Calorim.* **2007,** *90*, 849.
22. Aktas, L.; Altan, M. C. *Polym. Compos.* **2012,** *31*, 620.
23. Lin, T. K.; Kuo, B. H.; Shyu, S. S.; Hsiao, S. H. *J. Adhes. Sci. Technol.* **1999,** *13*, 545.
24. Vinayagamoorthi, S.; Vijayakumar, C. T.; Alam, S.; Nanjundan, S. *Eur. Polym. J.* **2009,** *45*, 1217.
25. Yei, D. R.; Fu, H. K.; Chen, W. Y.; Chang, F. C. *J. Polym. Sci. Polym. Phys.* **2006,** *44*, 347.
26. Tarase, M. V.; Zade, A. B.; Gurnule, W. B. *J. Appl. Polym. Sci.* **2010,** *116*, 619.
27. Budrugeac, P.; Segal, E. *Int. J. Chem. Kinet.* **2001,** *33*, 564.
28. Doyle, C. D. *J. Appl. Polym. Sci.* **1962,** *6*, 639.
29. Coats, A. W.; Redfern, J. P. *Nature* **1964,** *201*, 68.
30. Gorbachev, V. M. *J. Therm. Anal. Calorim.* **1975,** *8*, 349.
31. Agrawal, R. K.; Sivasubramanian, M. S. *J. Am. Chem. Eng.* **1987,** *33*, 1212.
32. Cai, J.; Yao, F.; Yi, W.; He, F. *J. Am. Chem. Eng.* **2006,** *52*, 1554.
33. Kandelbauer, A.; Wuzella, G.; Mahendran, A.; Taudes, I.; Widsten, P. *J. Appl. Polym. Sci.* **2009,** *113*, 2649.
34. Hao, W.; Hu, J.; Chen, L.; Zhang, J.; Xing, L.; Yang, W. *Polym. Test.* **2011,** *20*, 349.
35. Jankovic, B.; Adnadevic, B.; Jovanovic, J. *Thermochim. Acta* **2007,** *452*, 106.
36. Gao, W.; Cao, J. Z.; Li, J. Z. *Iran Polym. J.* **2010,** *19*, 255.
37. Vyazovkin, S.; Lesnikovich, A. *Thermochim. Acta* **1990,** *165*, 273.
38. Vyazovkin, S.; Burnhamb, A. K.; Criadoc, J. M.; Pérez-Maquedac, L. A.; Popescud, C.; Sbirrazzuolie, N. *Thermochim. Acta* **2011,** *520*, 1.
39. Hopewell, J. L.; Georgeb, G. A.; Hilla, D. J. T. *Polymer* **2000,** *41*, 8231.
40. Gao, W.; Cao, J.; Li, J. *Iran Polym. J.* **2010,** *19*, 959.
41. He, G. B.; Reidl, B.; Kadi, A. *J. Appl. Polym. Sci.* **2003,** *87*, 433.
42. Guigo, N.; Mija, A.; Vincent, L.; Sbirrazzuoli, N. *Phys. Chem. Chem. Phys.* **2007,** *9*, 5359.